

Original citation:

Bradley, M. K. (Matthew K.), Woodruff, D. P., Robinson, Jim, Dr. and Sheppard, Daniel Crispin. (2015) Adsorbate-induced surface stress, surface strain and surface reconstruction : CH₃S on Cu(100) and Cu(111). Surface Science, Volume 635 . pp. 27-36.

Permanent WRAP url:

<http://wrap.warwick.ac.uk/65511>

Copyright and reuse:

The Warwick Research Archive Portal (WRAP) makes this work of researchers of the University of Warwick available open access under the following conditions. Copyright © and all moral rights to the version of the paper presented here belong to the individual author(s) and/or other copyright owners. To the extent reasonable and practicable the material made available in WRAP has been checked for eligibility before being made available.

Copies of full items can be used for personal research or study, educational, or not-for-profit purposes without prior permission or charge. Provided that the authors, title and full bibliographic details are credited, a hyperlink and/or URL is given for the original metadata page and the content is not changed in any way.

Publisher statement:

NOTICE: this is the author's version of a work that was accepted for publication in Surface Science. Changes resulting from the publishing process, such as peer review, editing, corrections, structural formatting, and other quality control mechanisms may not be reflected in this document. Changes may have been made to this work since it was submitted for publication. A definitive version was subsequently published in <http://dx.doi.org/10.1016/j.susc.2014.12.003>

A note on versions:

The version presented here may differ from the published version or, version of record, if you wish to cite this item you are advised to consult the publisher's version. Please see the 'permanent WRAP url' above for details on accessing the published version and note that access may require a subscription.

For more information, please contact the WRAP Team at: publications@warwick.ac.uk




<http://wrap.warwick.ac.uk/>

Adsorbate-induced surface stress, surface strain and surface reconstruction: CH₃S on Cu(100) and Cu(111)

M.K. Bradley, D.P. Woodruff*, J. Robinson, D.C. Sheppard,
Physics Department, University of Warwick, Coventry CV4 7AL, UK

A. Hentz
Instituto de Física da UFRGS, Av. Bento Gonçalves 9500 - Porto Alegre, Brazil

Abstract

Density functional theory (DFT) calculations have been applied to study the structural phases formed by CH₃S on Cu(100) and Cu(111). On Cu(100) the results show that while the observed 0.25 ML (2x2) phase is stable, a faulted missing-row 0.33 ML c(6x2) is energetically preferred to a 0.5 ML c(2x2) phase, consistent with experimental observations. The calculations also show that a c(2x2) phase would have a large adsorbate-induced compressive surface stress that is not found in the c(6x2) phase. An alternative model of the c(6x2) phase as a buckled c(2x2) structure is shown to be unstable. On Cu(111), a 0.33 ML ($\sqrt{3} \times \sqrt{3}$)R30° structure on an unreconstructed surface is found to be less stable than a  reconstructed surface with the same coverage,

consistent with experimental data that the ($\sqrt{3} \times \sqrt{3}$)R30° phase is only seen at low temperatures and transforms to the reconstructed phase on heating. DFT calculations show that the originally-proposed pseudo-(100) structure for this reconstruction is heavily distorted, consistent with the results of other recent calculations. A range of alternative reconstruction models are found with closely similar total energies, the structural model with (marginally) the lowest energy having 20% less Cu adatoms in the reconstructed layer than in the ideal pseudo-(100) model. Simulations of medium energy ion scattering


* corresponding author. email d.p.woodruff@warwick.ac.uk; tel: +44 2476 523378

(MEIS) data for these different models show this lowest-energy model to give the best fit to the MEIS data, but the scattered-ion yield enhancement is sensitive to which of two alternative versions of this model, involving Cu adatoms predominantly in fcc or hcp sites, is occupied. The possible role of local disorder and structural variability in the surface, and whether the reconstruction could be incommensurate, is discussed.

Keywords: density functional theory; medium energy ion scattering; surface structure; surface reconstruction; copper; methyl thiolate

1. Introduction

It is now well-established that adsorption on surfaces can lead to significant modification of the structure of the outermost atomic layer(s) of the substrate material; in some cases, the resulting changes are quite subtle, involving small local atomic relaxations, but in others major reconstruction of the surface occurs. One class of adsorption structures in which significant adsorbate-induced reconstruction is believed to occur is in the interaction of alkane thiols with the (111) surfaces of the coinage metals, Cu, Ag and Au to form so-called self-assembled monolayers (SAMs) (e.g. [1]). The first clear evidence of this seems to have come from an investigation of the methylthiolate species, CH_3S^- , on Cu(111) in which both SEXAFS (surface extended X-ray absorption fine structure) and NIXSW (normal-incidence X-ray standing waves) measurements indicated that the S headgroup atom must penetrate the outermost Cu layer sufficiently to require substantial reconstruction [2]. In this initial study it was assumed that the hexagonal packing of the substrate was retained in the outermost reconstructed Cu layer, the thiolate species being bonded at three-fold coordinated sites, but a later STM (scanning tunnelling microscopy) investigation revealed a near-four-fold symmetry in the image [3]. This led to the suggestion that the surface undergoes a pseudo-(100) reconstruction, as found for some atomic adsorbate systems on fcc (111) and (110) surfaces [4], with the thiolate species being located in the four-fold coordinated hollow sites of this Cu layer to form a local

$c(2 \times 2)$ phase. In this model, suggested to involve a commensurate  phase

(defined relative to primitive translation vectors of the Cu(111) surface separated by the obtuse angle), the Cu-Cu nearest neighbour spacing is approximately 15% larger than in the (100) surface of bulk Cu. MEIS (medium energy ion scattering) measurements were found to be consistent with this commensurate model structure [5]. However, we should note that while the approximate dimensions of the surface mesh, as seen in STM, are consistent with this commensurate structure, this technique lacks the precision to confirm true commensuration. Indeed, the measured low energy electron diffraction (LEED) pattern may indicate that it is *not* truly commensurate [6]; this issue is discussed further

in section 4.

The known behaviour of methylthiolate on Cu(100) gives some support to the apparent energetic preference for a strained pseudo-(100) reconstruction on Cu(111). In particular, methyl thiolate has been found to form a 0.25 ML (2x2) structure on Cu(100) in which the S headgroup atoms do occupy four-fold coordinated hollow sites [7, 8]. On the other hand, most investigations conclude that methylthiolate does not form a stable 0.5 ML c(2x2) structure on Cu(100), but instead, at higher coverage than 0.25 ML, forms a c(6x2) phase. The c(6x2) phase has been observed on Cu(100) for a range of other alkanethiolate species, $\text{CH}_3(\text{CH}_2)_{n-1}\text{S}$, with different chain lengths ($n=2,4,6,7,10$) [9, 10, 11] (albeit with one suggestion that this phase may be metastable to partial dissociation [11]), and also for benzenethiolate [12]. However, methylthiolate overlayers do reveal small areas in STM images that appear to correspond to a c(2x2) phase [13] at room temperature, while a c(2x2) LEED pattern has been reported [14] with a sample temperature of 140 K during exposure to dimethyldisulphide (DMDS – $\text{CH}_3\text{S}=\text{SCH}_3$). One suggested reason for the apparent general preference for a c(6x2) phase rather than a c(2x2) phase is that the adsorbate-induced compressive surface stress of a long-range-ordered c(2x2) phase would be too large; the c(6x2) phase could correspond to a buckled c(2x2) phase such that this stress is relieved [13], although an alternative view is that the true coverage of this phase is less than 0.5 ML, involving a kind of vacancy-c(2x2) structure [9]. The idea that compressive surface stress generally precludes the formation of a c(2x2) phase on Cu(100) would be consistent with a c(2x2) phase forming in an *expanded* pseudo-Cu(100) reconstructed layer on Cu(111). Further support for the possible role of adsorbate-induced compressive surface stress comes from a MEIS study of the Cu(100)(2x2)- CH_3S phase that shows evidence of a small lateral outward strain of the Cu atoms bonded to the S headgroup atom [15]; this strain is symmetry-forbidden in a c(2x2) phase.


In order to cast further light on the structure of these phases, including the possible role of surface stress relief, we have undertaken a density functional theory (DFT)

investigation of the adsorption of CH_3S on $\text{Cu}(100)$ and $\text{Cu}(111)$. In particular, we have evaluated the relative total energies (and surface stresses on $\text{Cu}(100)$) in different structural models, and compared the lowest-energy structures with the results of experimental investigations into these surfaces. In the case of the $\text{Cu}(111)/\text{CH}_3\text{S}$ system, we also report the results of further modelling of the related medium energy ion scattering (MEIS) experimental data to test the experimental implications of the structures proposed here.

In fact there have been other recent DFT studies that address some of these aspects. Ferral *et al.* [16] reported a DFT study of methylthiolate and ethylthiolate on both $\text{Cu}(100)$ and $\text{Cu}(111)$ in 2006, but considered only possible adsorption structures that involved no substrate reconstruction; they did, however, report some relevant results on the structure (and local strain) in the $\text{Cu}(100)(2\times 2)\text{-CH}_3\text{S}$ phase. More recently, during the rather extended period of our own investigation, there have been two independent reports of DFT calculations relating to the methylthiolate-induced reconstruction of $\text{Cu}(111)$. The first of these [17] considered only the relaxation of the proposed pseudo-(100) reconstruction, but a further investigation, published as the present manuscript was originally being completed [18], has explored some alternative models for this reconstruction phase. Further discussion of the results of these parallel studies is presented below in comparison to our own conclusions.

2. Computational Details

The DFT calculations reported here were conducted using the plane-wave pseudopotential computer code CASTEP 5.501 [19]. The RPBE exchange-correlation functional [20] was used throughout along with ultrasoft pseudopotentials. A plane wave cut-off energy of 400 eV provided adequate basis set convergence, and relatively dense Monkhorst-Pack k-point meshes were needed, along with a Hellmann-Feynman force tolerance of 0.02 eV/\AA , to provide well-converged surface stresses in the double-sided surface slabs considered in the study of the (100) surfaces. Specifically, the k-point meshes were $16\times 16\times 1$ for (2×2) models using 9-layer double-sided slabs (with the

innermost three layers fixed at the parameters found for bulk Cu), and 8x12x1 for c(6x2) models on 5-layer double-sided slabs with only the middle one layer fixed to the bulk structure (with a Cu-Cu nearest-neighbour distance of 2.585 Å). For the Cu(111) calculations, focussed on structural optimisation rather than surface stress determination, 3-layer single sided slabs were used with k-point sampling of 12x12x1 for models described in a (2x2) mesh, 8x12x1 for a (3x2) mesh (used to calculate variations based on a ($\sqrt{3}\times\sqrt{3}$)R30° structure), and 2x2x1 and 6x6x1 for the models using the  mesh.

A vacuum gap of at least 14 Å was used to ensure minimal interaction between slabs.

The adsorption energy per CH₃S species on Cu(100) (using double-sided slabs) referenced to a gas-phase molecule of DMDS is defined as

$$E_{ad-CH_3S} = -\frac{1}{2N_{CH_3S}} \left(E_{substrate+CH_3S} - E_{substrate} - N_{CH_3S} E_{DMDS} \right)$$

where N_{CH_3S} is the number of methylthiolate species per unit mesh on each surface. We also define a surface energy change per (1x1) unit mesh associated with the adsorption as

$$E_{ad-CH_3S}^* = -\frac{1}{2A} \left(E_{substrate+CH_3S} - E_{substrate} - N_{CH_3S} E_{DMDS} \right)$$

where A is the area of each face of the unit mesh in units of the (1x1) substrate mesh. This parameter provides a more meaningful method of comparing the energy of structures with different thiolate coverages. Notice that both of these energies are defined such that a positive value corresponds to a reduction in total energy and is thus energetically favoured. With both faces of the slabs having identical adsorbate coverage the surface stress is the same on each face, and it is particularly trivial to extract this quantity from the calculated three-dimensional stress tensor, computed within CASTEP according to the so-called stress theorem [21].

For the calculations of CH₃S on Cu(111), involving a reconstructed surface layer containing N_{Cu} Cu adatoms per unit mesh, and performed on single-sided slabs, these definitions are modified to

$$E_{ad-CH_3S} = -\frac{1}{N_{CH_3S}} \left(E_{substrate+CH_3S} - E_{substrate} - N_{Cu} E_{Cu-bulk} - \frac{1}{2} N_{CH_3S} E_{DMDS} \right)$$

and

$$E_{ad-CH_3S}^* = -\frac{1}{A} \left(E_{substrate+CH_3S} - E_{substrate} - N_{Cu} E_{Cu-bulk} - \frac{1}{2} N_{CH_3S} E_{DMDS} \right)$$

Where $E_{Cu-bulk}$ is the energy per Cu atom in bulk solid Cu.

3. Results

3.1 Methylthiolate on Cu(100)

Table 1 summarises the main findings of the calculations of methylthiolate structures on Cu(100). For the 0.25 ML (2x2) phase the S headgroup, as expected, is found to occupy the 4-fold-coordinated hollow sites with the S-C bond almost exactly perpendicular to the surface and a Cu-S bondlength of 2.34 Å. Calculations starting with the molecular axis tilted relative to the surface normal converged on this single structure with the molecule upright. This structure is in reasonable agreement with the experimental studies which show the molecule to be tilted by $10 \pm 10^\circ$ with a Cu-S bondlength of 2.29 ± 0.03 Å [7, 8] (a value almost identical to that found for the $n=6, 12$ and 16 alkane thiolates [22]). This structure also shows a lateral displacement of the Cu atoms bonded to the S headgroup by 0.04 Å. This qualitative effect is consistent with the experimental results of the MEIS study [15], although the experimental value of 0.12 ± 0.04 Å is significantly larger. The earlier DFT study of Ferral *et al.* [16] led to the same value as in the present calculations.

The small energetic preference for the S-C bond to be tilted in the c(2x2) phase is also consistent with these earlier DFT results. An important new result in Table 1, however, is the calculated surface stress. On the clean surface the calculations yield a tensile stress of 2.06 Nm^{-1} , similar to the value of 1.89 Nm^{-1} found in the earlier calculations of Harrison *et al.* [23] using a different functional. Adsorption of 0.25 ML methylthiolate leads to a significant reduction of this tensile stress, while in the c(2x2) 0.5 ML phase the surface stress becomes strongly compressive, although the tilting of the molecules does lower this compressive stress significantly relative to the (slightly less energetically favourable)

model in which the molecular axes are upright. Despite this surface stress, however, the c(2x2) phase is energetically favourable; the adsorption energy per adsorbate species falls, relative to the lower-coverage phase, but there is a marginal increase in the surface energy change per unit area.

As noted above, experimentally, there is no evidence that a long-range ordered c(2x2) phase actually occurs, at least at room temperature, but instead that increased coverage beyond 0.25 ML leads to a c(6x2) phase which appears to correspond to saturation. This would imply that this larger surface mesh structure should have a lower energy than the c(2x2) phase. We have therefore investigated possible structural models for this phase. One suggestion, mentioned above, is that the c(6x2) phase is actually a strained c(2x2) structure, with a coverage of 0.5 ML, the large compressive stress of the c(2x2) phase leading to a periodic buckling of the surface [13]. The results of our calculations, however, do not support this model; a series of calculations, initiated from buckled c(6x2) models, all converged on the ideal c(2x2) structure. The alternative model, proposed in the context of a study of hexanethiolate in Cu(100) [9], is that the c(6x2) structure is a faulted missing-row version of the c(2x2) structure. The lowest-energy configuration of this model for methylthiolate adsorption, found in our study, is shown in Fig. 1. This structure has a methylthiolate coverage of 0.33 ML, broadly consistent with the value of 0.3 ML found in experiments on the c(6x2)-hexanethiolate phase [9]. As shown in Table 1, this structure is very significantly favoured energetically over the c(2x2) phase; a transition from this structure to the higher-coverage c(2x2) structure would involve a significant decrease in $E_{ad-CH_3S}^*$ and so would not be expected to occur. On the other hand, the adsorption energy per thiolate species is larger in the (2x2) phase than in the c(6x2) phase. The results are thus fully consistent with the formation of a (2x2) phase at low coverage, a c(6x2) phase at higher coverage, but no progression to the even higher coverage c(2x2) phase.

Table 1 also includes the structural parameters associated with the c(6x2) structure. There appear to have been no experimental quantitative structural studies of the c(6x2) methylthiolate phase, but a SEXAFS study of the equivalent hexanethiolate phase found

the Cu-S distances to be 2.28 ± 0.02 Å [9]; in the DFT structure the slightly asymmetric (off-hollow) bonding sites lead to Cu-S bondlengths in the range 2.29-2.42 Å. One piece of experimental information that is available for the $c(6 \times 2)$ methylthiolate phase is the STM image, an extract of which is shown in Fig. 1 compared with the simulated image derived from the DFT calculations using the usual Tersoff-Hamann [24] approach. At first glance the simulated and experimental images look rather different. In particular, while the experimental images show single broad protrusions with the $c(6 \times 2)$ periodicity, in the simulated image the main features are partially-resolved double-protrusions, corresponding to pairs of methylthiolate species. It is important to recognise, however, that the experimental image represents a time average of all molecular free and frustrated rotational vibrations of the molecules, which occur on a much faster time-scale than the imaging, while the simulated image is of the static structure. A substantial smearing must therefore be applied to the simulated image to make the comparison meaningful. The discrepancies under these circumstances are far less significant, although the simulated image would lead one to expect that the single protrusions seen in the experimental images would be more elongated than those that are actually observed.

3.2 Methylthiolate on Cu(111)

3.2.1 DFT structures and STM images

As described in the introduction, the stable ordered phase of methylthiolate on Cu(111) at room temperature is generally accepted to correspond to a large surface mesh reconstruction. The originally-proposed model for this phase is a $c(2 \times 2)$ methylthiolate overlayer on a strained pseudo-(100) reconstructed Cu layer, with the S headgroup atoms occupying 4-fold coordinated hollow sites. This basic model is shown in Fig.2, with the Cu atoms in the reconstructed layer drawn with a much smaller radius than the substrate atoms to allow the relationship between the overlayer and substrate meshes to be seen more clearly. The lateral registry of the overlayer and substrate in this diagram is arbitrary. In the original STM paper in which this structure was first proposed [3], it was suggested that the structure (assuming it is commensurate with the substrate) could be

described in the matrix notation as $\begin{bmatrix} 5 & 0 \\ 1 & 3 \end{bmatrix}$ relative to the substrate primitive translation vectors (PTVs) separated by an angle of 60° . This oblique unit mesh is shown in Fig. 2 by the black lines. Insofar as crystallographic convention for a hexagonal structure is that the substrate should be described by the PTVs separated by an obtuse angle (120°) this mesh is more correctly denoted as $\begin{bmatrix} 5 & 0 \\ 4 & 3 \end{bmatrix}$. Subsequently, this overlayer structure has been more commonly described [5] by the near-square unit mesh shown as white lines in Fig. 2, denoted in the standard crystallographic convention by the matrix $\begin{bmatrix} 4 & 3 \\ 3 & 3 \end{bmatrix}$.

Notice that these are two alternative ways of describing exactly the same overlayer periodicity; a recent publication [18] has implied that these are different structures, but this seems to be due to a misunderstanding regarding the use of acute or obtuse angles in the substrate PTVs.

Calculations were initially undertaken for this ideal pseudo-(100) reconstructed surface, but also for simple overlayer phases on an unreconstructed Cu(111) surface. In particular, calculations were performed on a 0.25 ML (2x2) phase, and on several different 0.33 ML phases including a simple $(\sqrt{3} \times \sqrt{3})R30^\circ$ phase, but also variations of this phase in which the molecules lie at the sites of a $(\sqrt{3} \times \sqrt{3})R30^\circ$ mesh but have different tilt azimuths of the thiolates, leading to a larger (3x2) unit mesh. The simple $(\sqrt{3} \times \sqrt{3})R30^\circ$ phase was found to have a lower energy than these (3x2) modifications, and indeed is also energetically favoured (largest value of $E^*_{ad-CH_3S}$) over the lower-coverage (2x2) phase, as shown in Table 2. In both phases the S headgroup atom lies in an off-hollow site, displaced towards the bridging site, the C-S bond being tilted relative to the surface normal by 33° in the $(\sqrt{3} \times \sqrt{3})R30^\circ$ phase and by 47° in the (2x2) phase. These conclusions are in excellent agreement with the results of Feral *et al.* [16] who investigated only these unreconstructed models. There is one report of the observation of a Cu(111) $(\sqrt{3} \times \sqrt{3})R30^\circ$ -CH₃S phase at low temperatures (110-140 K) [6], but at room

temperature this transforms to the $\begin{smallmatrix} 4 \\ \text{M} \\ 3 \end{smallmatrix} \begin{smallmatrix} 3 \\ \{ \\ 3 \end{smallmatrix}$ phase, suggesting that the $(\sqrt{3} \times \sqrt{3})R30^\circ$ phase is metastable and reconstructs with the aid of thermal activation. Calculations for a 0.5 ML (2x1) phase failed to find any stable adsorption structure, the molecules simply moving off the surface as the structural optimisation calculation progressed.

Relaxation of the ideal pseudo-(100) reconstruction model to minimise the energy led to very significant displacements of the Cu atoms within the reconstruction, and this structure, labelled ‘reconstruction A’ in Table 2, has a lower energy (higher value of $E_{ad-CH_3S}^*$) than the unreconstructed $(\sqrt{3} \times \sqrt{3})R30^\circ$ (with the same thiolate coverage of 0.33 ML), consistent with the higher stability of the $\begin{smallmatrix} 4 \\ \text{M} \\ 3 \end{smallmatrix} \begin{smallmatrix} 3 \\ \{ \\ 3 \end{smallmatrix}$ phase found in experiments.

This heavily-relaxed pseudo-(100) reconstruction is shown in Fig. 3 and appears to be essentially the same as that originally found by Grönbeck [17] and more recently also obtained by Seema *et al.* [18]. A key feature of this structure is that 60% of the S headgroup atoms retain the 4-fold coordination of the original pseudo-(100) structure, but the remaining 40% of these atoms have 3-fold coordination to the Cu atoms in the reconstructed layer. Calculations starting from different overlayer-substrate registries in the pseudo-(100) model all led to reconstruction A, with only minor variations in the methyl-group rotations. All of these structures yielded total energies within 1 meV/(1x1) unit mesh of the most energetically-favourable reconstruction A model.

One key structural parameter of this model that can be compared with the results of NIXSW experiments is the average height of the S headgroup atoms above the outermost unreconstructed Cu(111) layer. The NIXSW experiments [2] led to a value of the (111) coherent position of 1.20 ± 0.10 Å, which corresponds to the height above the nearest *extended* bulk layer. Adding one bulk layer spacing of 2.08 Å gives the height of the S atoms above the outermost unreconstructed layer of 3.28 ± 0.10 Å which is in good agreement with the average value found for reconstruction A of 3.22 Å (the range of the five different values within the unit mesh being 0.13 Å). However, one significant


implication of the relaxation of the pseudo-(100) model, in which many of the Cu adatoms in the reconstructed layer move towards bulk termination sites, is that we may anticipate that this model will significantly degrade the level of agreement with the experimental MEIS data, as evaluated in the following section. In part because of this, we have explored a range of alternative reconstruction models.

While the original pseudo-(100) model clearly defines the number of Cu adatoms in the reconstructed layer as 10 per surface unit mesh (compared to 15 Cu atoms in each underlying substrate layer within the same unit mesh), if the pseudo-(100) layer is very strongly distorted, as in reconstruction A, there is no obvious reason for retaining this constraint. In order to search for alternative lower-energy solutions, a range of new models were explored with fewer (8 or 9) or more (11 or 12) Cu atoms per unit mesh within the reconstructed layer. These models were mostly initiated from variations of the pseudo-(100) structure by removing or adding Cu atoms (the added atoms initially placed in hollow sites not occupied by thiolate species). In order to allow a reasonable range (12) of structures to be explored in a reasonable time, these initial searches were performed using a coarser (2x2x1) k-point sampling mesh. While comparisons of adsorption energies between the calculations using 2x2x1 and 6x6x1 sampling are unlikely to be wholly reliable, we would expect comparisons of the energies of different models with the same 2x2x1 sampling to be sufficiently meaningful to identify the lowest energy structures; these models were then reoptimised using the finer k-point sampling. A summary of the more favourable structures is given in Table 3. Many of these structures were found to have adsorption energies a few tens of meV less favourable than reconstruction A, but one model, reconstruction G (see Fig. 4) was found to be very fractionally favoured over reconstruction A, with an adsorption energy per thiolate species (using 6x6x1 k-point sampling) that was 6 meV more favourable (Table 2); such a small energy difference, of course, can be no more than marginally significant in view of the limited accuracy of DFT calculations.

As shown in Fig. 4, reconstruction model G has only 8 Cu adatoms per unit mesh in the reconstructed layer, leading to a structure in which only 20% of the thiolate species (one

per unit mesh) are 4-fold coordinated to the Cu atoms, while the remaining 80% are 3-fold coordinated to these Cu atoms. The thiolate species in these majority sites have S-Cu distances to these underlying unreconstructed Cu layer atoms of ~ 3.2 Å (compared to ~ 2.3 - 2.4 Å to the Cu adatoms), so the bonding is clearly dominated by 3-fold coordination in the reconstructed layer. Evidently the driving force for the reconstruction is *not* a preference for 4-fold coordination, as might have been implied by the ideal pseudo-(100) reconstruction model. Notice that the average height of the S head-group atoms above the outermost unreconstructed Cu layer is 3.12 Å, slightly lower than for reconstruction model A but still in reasonable agreement with the NIXSW experimental value.

A common feature of these models, of course, is that the arrangement of the Cu adatoms in the reconstructed layer is far from the near-square arrangement of the pseudo-(100) model that was inferred from the STM images. However, the periodicity of the regular protrusions in the STM image is consistent with them corresponding to the location of the thiolate species, not the Cu adatoms, and inspection of both the reconstruction models of Figs. 3 and 4 shows that the thiolate species are arranged in an approximately square pattern. Confirmation of this is provided by simulations of the STM image produced from the DFT calculations and shown in Fig. 5, together with a similar area of the experimental STM image extracted from ref. [3]. The simulated STM images from both model structures do, indeed, show protrusions arranged on a near-square grid, although there are underlying corrugations that lead to a range of different protrusion heights such

that the larger  periodicity can easily be discerned. No such systematic height variation is evident in the experimental images, but the level of noise and the observation of height (brightness) variations that show no evidence of periodicity suggests that it would be difficult to observe the variations seen in the simulations with this image quality. As for the (100) surface, we also note that these STM image simulations correspond to a static structure, while the experimental image represents a time average of the (fast) rotational and vibrational (including wagging) modes of the molecules on the surface. These dynamic effects will certainly lead to both lateral and perpendicular

smearing of the simulated images. Bearing in mind these limitations, we may conclude that the STM simulations for both the (111) surface reconstruction models are consistent with experiment.

3.2.2 MEIS simulations

One important piece of experimental information that had previously been found to support the pseudo-(100) reconstruction model of the $\sqrt{3} \times \sqrt{3}$ phase is the 100 keV H^+ medium ion scattering results of Parkinson *et al.* [5]. In view of the strong modification of this structure found in all the DFT studies, it is important to consider whether the relaxed reconstruction A is consistent with these data, and whether the experimental MEIS data provide a basis for distinguishing the alternative models that are found to have closely-similar total energies in the DFT calculations.

The MEIS technique [25] is closely related to the standard method of materials analysis of Rutherford backscattering, but the use of somewhat lower energies offers advantages for studies of near-surface crystallography. The energy of the elastically-scattered ions from the surface in a particular direction identifies the atomic mass of the scatterer atom, but by using incidence along a low index crystallographic direction, the shadow cones produced by the scattering from the outermost layer(s) shadow deeper-lying atoms and lead to a highly surface-specific signal. In principle one can arrange to illuminate only one, or two, or some other specific small number of layers by choosing appropriate crystallographic directions; in practice thermal vibrations lead to some small visibility of deeper layers. Surface structural data is obtained by measuring so-called blocking curves that comprise the scattered ion yield as a function of scattering angle for a fixed incidence direction. The same shadowing effect occurs in the outgoing trajectories of ions scattered from subsurface layers, leading to ‘blocking dips’ in the yield at angles corresponding the alignment of the outgoing trajectory with the location of atoms closer to the surface. One further particularly important feature of the technique in the present context is that the scattering yield can be calibrated in an absolute fashion, so one can determine exactly

how many layers contribute to the signal. Thus, if near-surface atoms of the substrate species are displaced from their ideal bulk-termination sites, they lead to enhanced illumination of underlying atoms with a consequential increase in the scattered ion yield. It is this feature that is particularly useful in studying the surface reconstruction discussed here. Specifically, the technique provides a method of determining how many Cu atoms lie in the reconstructed surface layer, providing that these atoms are sufficiently displaced from bulk-termination positions. Of course, the reconstruction in the surface layer also leads to some movement of atoms in the outermost underlying ‘bulk’ layers, which can also lead to slightly-enhanced scattering yields.

Fig. 6 provides some information on the size and distribution of the lateral offsets of Cu atoms, relative to a bulk-termination structure, in the reconstructed overlayer and in the outermost two substrate layers, for several of the different reconstruction models identified in Table 3. The visibility enhancement induced by atomic displacements (and their associated vibrational amplitudes) is determined by the shadow cone radius which, for 100 keV H^+ scattering from Cu atoms at typical interatomic distances is $\sim 0.17 \text{ \AA}$, so a displacement much less than this will lead to minimal enhancement of the scattered ion yield, while a displacement significantly larger than this will lead to an enhancement equivalent to the scattering from one Cu atom. Displacements of intermediate size will lead to partial enhancement of the scattered ion signal.

These differences are reflected in the simulations of the experimental blocking curves [5] performed using the VEGAS computer code [26], as shown in Fig. 7; for clarity this figure shows only simulations for the clean surface, the ideal pseudo-(100) reconstruction, models A and G, and modified versions of these two structures described below. The figure shows data collected using two different incidence directions that correspond to nominal illumination of only one or two layers of a bulk-terminated Cu(111) surface, although the peak scattered-ion yields (expressed in terms of the number of contributing layers) are higher than these nominal values of 1 and 2 due to the effects of atomic vibrations and surface relaxations as well as the reconstruction. The dips in the curves correspond to blocking in certain directions of ions scattered from the lower

layers. The experimental data from the clean Cu(111) surface is well-fitted by the VEGAS simulations, as reported previously [5]. The simulations for the ideal pseudo-(100) reconstruction model give a good fit to the data from the thiolate-covered surface, as previously reported; the simulations shown here differ very slightly from those reported previously [5], which failed to take account of the need to average over the three distinct rotational domains of the surface structure arising from the 3-fold symmetry of the substrate, but the overall agreement between experiment and theory is very similar. As expected, the scattered-ion yield increases in the presence of the thiolate due to the fact that the Cu atoms in the reconstructed layer no longer occupy bulk-termination sites. However, the simulations for model A, which is the fully relaxed modification of the pseudo-(100) model, show much lower Cu scattering yields. Indeed, the simulations for this model show far better agreement with the experimental data from the clean surface than those from the thiolate-dosed surface. The reason for this is clear; optimising the geometry to minimise the total energy leads to the Cu adatoms moving closer to the three-fold coordinated hollow sites on the underlying substrate that are (mostly) bulk-termination sites. The fact that the calculated yield at high scattering angles in the 2-layer incidence geometry are almost identical to those for the clean surface is superficially surprising, but can be attributed to the larger vibrational amplitudes of the outermost Cu atoms in the clean surface [27], which are assumed to be suppressed in the presence of the reconstructed overlayer.

Simulations for several of the other reconstruction models (not shown) give somewhat larger predicted scattered ion yields than those of model A, but reconstruction G gives the highest yield at most scattering angles. This model actually contains 20% less Cu adatoms per unit mesh than model A, but more Cu atoms show large displacements from bulk terminations sites, as shown in Fig. 6; the smaller number of adatoms is apparently more than compensated by the larger displacements of these atoms from the bulk-termination sites.

While reconstruction model G gives a significantly better fit to the experimental MEIS yields than model A, the simulated scattered ion yield enhancement as a result of the

thiolate deposition is still too small. One possible source of this discrepancy is the role of surface vibrations, but tests varying these amplitudes within reasonable limits failed to influence the simulation results significantly. Additional 4-layer DFT calculations were performed to allow three (rather than two) outermost substrate layer atomic positions to relax, in order to establish if deeper-layer relaxations may influence the scattered-ion yields, but feeding the results of these calculations into the MEIS simulations had very little effect on the blocking curves. However, closer inspection of models A and G reveals an alternative possible reason for this discrepancy. In particular these models have a significant fraction of the Cu adatoms close to the ‘fcc’ three-fold coordinated hollow sites (directly above a third layer substrate atom) that corresponds to those of a bulk termination. Adatoms close to bulk continuation sites will lead to very little enhancement of the MEIS yield. However, a general feature of fcc(111) surfaces is that the adsorption energy of many adsorbates that favour hollow sites is closely similar for these fcc hollows and for the alternative ‘hcp’ hollows directly above second layer substrate atoms. These hcp sites are, of course, far displaced laterally (by 1.47 Å) from the bulk-termination fcc sites. Most adsorbates have been found to prefer fcc hollows over hcp hollows, but the energy difference in DFT calculations is usually calculated to be very small, and indeed some adsorbates do prefer hcp hollow site occupation. Indeed, in the case of the unreconstructed Cu(111) clean surface, displacing *all* the outermost layer of Cu atoms from fcc to hcp hollows (creating a stacking fault at the first/second layer interface) has been calculated to cost only 41 meV per (1x1) unit mesh [28]. We have therefore explored alternative versions of models A and G in which the reconstructed layer is translated laterally across the surface such that more Cu adatoms lie near hcp sites. Specifically, in the unit mesh of the original model A there are 6 Cu adatoms near fcc hollows and 4 Cu adatoms near hcp hollows, while in the original model G there are 5 Cu adatoms near fcc hollows and 3 Cu adatoms near hcp hollows. In the modified ‘hcp’ versions of these models these fcc/hcp occupation numbers are reversed. The fully relaxed version of the modified model ‘hcpA’ has an E^* value 9 meV less favourable than the original model A, while the E^* value for the ‘hcpG’ model is actually 2 meV more favourable than the original model G. As shown in Fig. 6, these ‘hcp’ models involve far more Cu adatoms with large lateral displacements from bulk

continuation sites and as a result show substantially larger Cu scattered ion yields in MEIS simulations (fig. 7), particularly for the ‘hcpG’ reconstruction model for which the level of experiment/theory agreement is only slightly worse than the original (now seen to be unphysical) pseudo-(100) model.

Despite this much-improved agreement with the MEIS data for the ‘hcpG’ model, it is appropriate to consider if there may be possible sources of further enhancements scattered-ion yields that we are unable to test in VEGAS simulations. One is the role of disorder. We would certainly expect additional Cu adatom displacements at antiphase domain boundaries in the overlayer, but in addition the fact that many different model structures (containing different numbers of Cu adatoms) have closely similar total energies leads us to expect that the true surface phase may well involve some mixture of these different (local) structures, and that the associated disorder may lead to more Cu atoms being in sites that are further displaced from bulk-termination sites. Indeed, with so many different structures having almost the same total energy, all requiring substantial Cu adatom mobility to form, it is highly improbable that a perfectly-ordered single-phase surface can be formed experimentally.

A second possibility is that the surface reconstruction is not truly commensurate with the substrate. An incommensurate overlayer would almost certainly lead to more Cu adatoms being displaced further from bulk-termination sites. Modelling the consequences of incommensuration is, however, intractable computationally, and even using a massively-enlarged unit mesh to simulate this effect is beyond our computational resources. However, in view of the relaxation behaviour we have identified in the

relatively small commensurate $\begin{matrix} 4 & 3 \\ \text{M} & \{ \\ 4 & 3 \end{matrix}$ mesh it seems likely that a nominally incommensurate overlayer would actually relax to locally commensurate structures very similar to those identified here, albeit with distortion at boundaries between these local structures that may involve more highly-displaced Cu adatoms.

4. General discussion and conclusions

The results of our DFT calculations for the Cu(100)(2x2) and c(2x2)/CH₃S structures are consistent with those of earlier such calculations but provide some important new insights. In particular they show that a large compressive surface stress would be associated with the formation of a c(2x2) phase, although if one considers only the results for these two phases the DFT results would imply that a c(2x2) phase might be energetically preferred (the surface energy change for the c(2x2) phase is 6 meV/(1x1) unit mesh more favourable). However, our calculations for the c(6x2) phase, assuming a faulted-missing row structure with a coverage of 0.33 ML, clearly show that increasing the coverage to 0.5 ML to form a c(2x2) phase is *not* energetically favoured, as it would lead to a decrease in the (negative) surface energy change per unit surface area. Interestingly, this c(6x2) phase is found to have almost zero surface stress. Our calculations also indicate that the c(6x2) phase cannot be reconciled with a buckled c(2x2) structure, which we find to be unstable. The simulated STM images for the faulted-missing-row model do appear to show more atomic-scale detail than is evident in the experimental images, but at least part of this discrepancy may be attributed to the effects of surface vibrations and the problem of noise in the experimental images.

Our results for the Cu(111)/CH₃S reconstructed surface show, in agreement with the previous studies of Grönbeck [17] and Seema *et al.* [18], that the pseudo-(100) reconstruction model is significantly modified by surface relaxations, the resulting structure having S headgroup atoms in a mixture of 4-fold and 3-fold coordinated sites, rather than only 4-fold coordinated sites as in the ideal pseudo-(100) model. This result led Seema *et al.* to conclude that this structure cannot be consistent with the STM images that show a near-square arrangement of protrusions. Our STM simulations show that this assertion is clearly not correct, and that the simulated images are in rather good agreement with experiment. Despite the Cu adatom arrangement in this model being far from square-like, the thiolate species do retain this approximate periodicity, and it is these species that are imaged in STM.

In comparing our results with those of Seema *et al.* we should also note one further issue.

We have focussed on reconstruction models based on the $\begin{pmatrix} 4 & 3 \\ 1 & 3 \end{pmatrix}$ mesh, defined relative to PTRs of the substrate separated by the obtuse angle of 120° , the usual crystallographic convention. Seema *et al.* explored this same periodicity described by a $\begin{bmatrix} 5 & 0 \\ 1 & 3 \end{bmatrix}$ mesh based on substrate mesh PTRs separated by the acute angle of 60° , but also tested models based on a $\begin{pmatrix} 4 & 3 \\ 1 & 3 \end{pmatrix}$ also using substrate mesh PTRs separated by the acute angle of 60° .

This periodicity is not consistent with the experimentally-observed STM images and LEED pattern, but may perhaps have been used due to a misunderstanding of the different crystallographic conventions.

While the two most energetically favoured structural models, A and G, that we initially identified for the thiolate-induced reconstruction of Cu(111), yield simulated STM images that are consistent with the experimental images, neither model fits the MEIS data well. The ideal pseudo-(100) structure provides a much better fit to the MEIS data but, as established by three independent DFT studies, this structure clearly cannot occur in practice. However, the laterally-displaced alternative versions of these models, in which the majority of the Cu adatoms relax to locations close to hcp, rather than fcc, hollows do yield MEIS simulations in much better agreement with the experimental data. Indeed, the best agreement is for the ‘hcpG’ model which also has the lowest surface energy, albeit by only a few meV per (1x1) unit mesh. However, with so many structures having closely similar surface (a result also found by Seema *et al.* [18]), it is unlikely that a real surface will comprise only a single perfect structure, but will either have local regions of different structures or faulted versions of the most favourable structure(s). Nevertheless, the ‘hcpG’ model does give the best fit to the MEIS data, and does have the lowest energy, so it seems likely that minor variations of this structure are formed on much of the surface.

One final issue concerns the question of whether the overlayer reconstruction is actually

commensurate with the underlying substrate. This is important not only because all the DFT calculations are based on a commensurate overlayer, and become untenable for an incommensurate overlayer, but also because an incommensurate overlayer may be expected to lead to a significantly larger scattered-ion yield in MEIS. Of course, simulating MEIS data from an incommensurate overlayer is not achievable for similar reasons. The initial suggestion that the reconstruction may be commensurate was based on STM images of the overlayer alone (with no areas of imaged clean surface). Such images certainly lack the precision to establish, through measurement of the lateral spacings of the protrusions alone, whether a surface is or is not commensurate. If a structure is truly commensurate one may expect some rumpling of the overlayer with a period corresponding to that of the commensurate mesh, as is seen in the simulated STM images of Fig. 5. The experimental images do not show this effect, but the image quality is such that it is difficult to know if the absence of such a longer-range periodicity in the images is significant. A potentially more precise method of determining the presence or absence of commensuration is a conventional diffraction technique which shows, simultaneously, the periodicity of the substrate and the overlayer. The only such data available appear to be the LEED patterns of Driver and King [6] who remark that ‘very close inspection of the spot positions shows that certain of the fractional order beams lie at slightly higher angles than expected’ for the commensurate phase. Our own inspection of their published LEED pattern (Fig. 6(b) of ref. [6]) seems to confirm this view, with fractional order beams lying roughly midway between the first-order integral beams having locations indicative of an overlayer mesh up to 5% smaller than the proposed commensurate values. However, the diffraction patterns do not show any radial streaking or splitting of these integral order beams which would be expected to occur if the reconstructed overlayer is incommensurate, due to the mismatch of the substrate and overlayer unit meshes. The apparent displacement of the fractional order beams may, therefore, be due to a distortion in the recorded pattern (a problem that is common in recorded LEED patterns), rather than to incommensuration. A more quantitative diffraction investigation of the surface mesh would certainly be of interest. Note that Seema *et al.* actually conclude, on the basis of the results of their DFT calculations, that the overlayer may be incommensurate. However, this conclusion appears to be based on

the idea that the commensurate structures found (such as model A) are inconsistent with STM images; our own results show that this is not correct.

Structural parameters for the lowest-energy Cu(100) (2x2) and c(6x2) models, and the Cu(111) ‘hcpG’ model are provided in the Supplementary Material file Structure.txt.

Acknowledgements

The computing facilities were provided by the Centre for Scientific Computing of the University of Warwick with support from the Science Research Investment Fund.

Tables

Surface phase	model	E_{ad-CH_3S} (eV)	$E^*_{ad-CH_3S}$ (eV)	S_x (Nm ⁻¹)	S_y (Nm ⁻¹)	r_{Cu-S} (Å)	z_{Cu-S} (Å)	Δ_{xy} (Å)/ tilt (°)
(2x2)	upright	1.002	0.251	0.91	0.91	2.34	1.42	0.04/ 1.0
	tilted	becomes upright	-	-	-	-	-	-
c(2x2)	upright	0.487	0.244	-3.36	-3.36	2.32	1.43	-/ 0.1
	tilted	0.513	0.257	-2.39	-1.95	2.31/2.44	1.51	-/ 27.9
c(6x2)	missing row	0.889	0.296	-0.02	0.08	2.29-2.42	1.36-1.49	0.07/ 7.9/3.3
(1x1)	clean	-	-	2.06	2.06	-	-	-

Table 1. Summary of the main energetic and structural properties of the lowest energy structures found for CH₃S on Cu(100).

Phase	CH ₃ S coverage (ML)	Cu coverage (ML)	E_{ad-CH_3S} (eV)	$E^*_{ad-CH_3S}$ (eV)
(2×2)	0.25	-	0.586	0.147
(2x1)	0.5	-	unstable	-
($\sqrt{3}\times\sqrt{3}$)R30°	0.33	-	0.487	0.162
reconstruction A	0.33 (5/15)	10/15	0.529	0.176
reconstruction G	0.33 (5/15)	8/15	0.535	0.178

Table 2. Summary of the relative energies of the lowest energy structures found for CH₃S on Cu(111).

reconstruction	Cu coverage (ML)	E_{ad-CH_3S} (eV)	$E_{ad-CH_3S}^*$ (eV)
A	10/15	0.511	0.170
E	11/15	0.493	0.164
F	9/15	0.489	0.163
G	8/15	0.509	0.170
H	8/15	0.487	0.162
I	11/15	0.381	0.127
J	12/15	0.395	0.132

Table 3. Summary of the relative energies of some more favourable $\sqrt{3} \times \sqrt{3}$ structures found for CH₃S on Cu(111) using reduced 2x2x1 k-point sampling.

Figure Captions

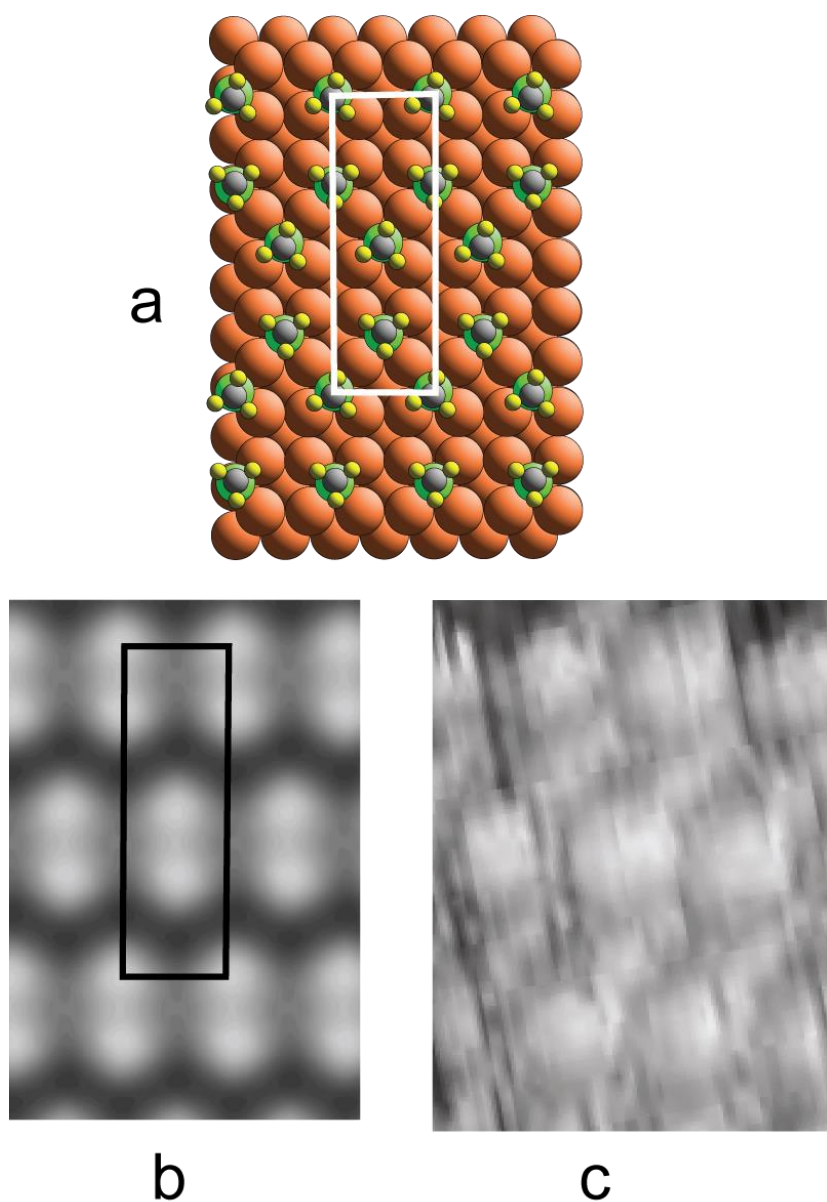


Fig. 1 (a) shows a schematic plan view of the lowest-energy structural model found for the Cu(100)c(6x2)-CH₃S structure, while (b) shows a simulated STM image. An experimental STM image, extracted from ref [13] is shown in (c). In (a) the Cu atoms are shown as the largest (gold-coloured) spheres while the S, C and H atoms shown with successively decreasing sizes are coloured green, grey and yellow, respectively.

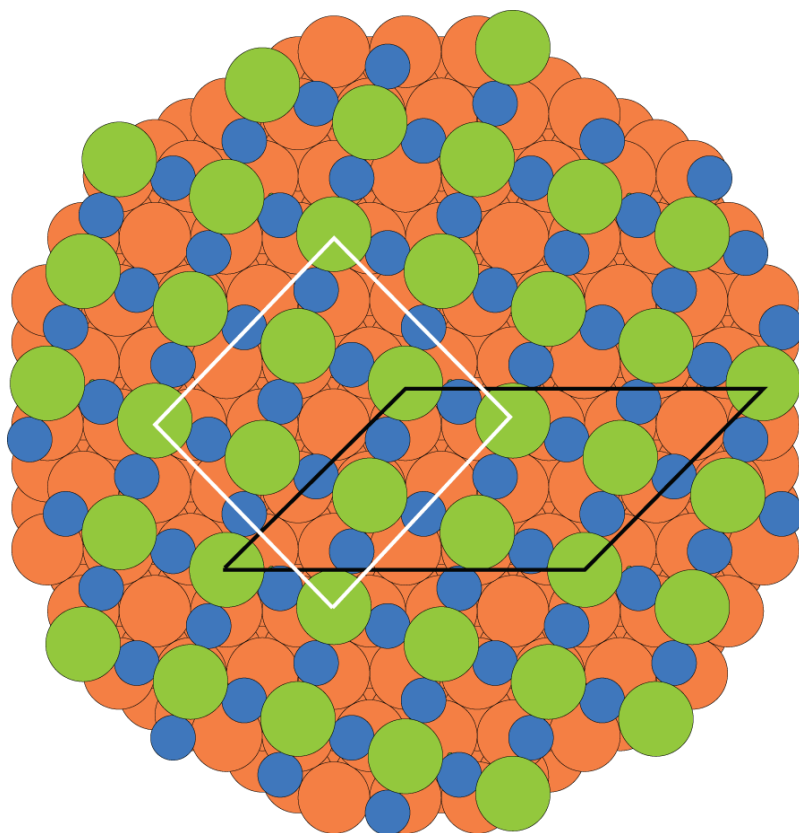


Fig. 2. Plan view of the basic pseudo-(100) reconstruction model of Cu(111) induced by methylthiolate adsorption. The Cu atoms in the reconstructed overlayer are shown as small (blue) circles to allow the position of the underlying unreconstructed Cu atoms (gold) to be seen. The methylthiolate adsorbates are represented by their S headgroup atoms as large (green) circles. The lateral registry of the overlayer and substrate in this diagram is arbitrary. Two alternative unit meshes, described in the text, are superimposed on the structure.

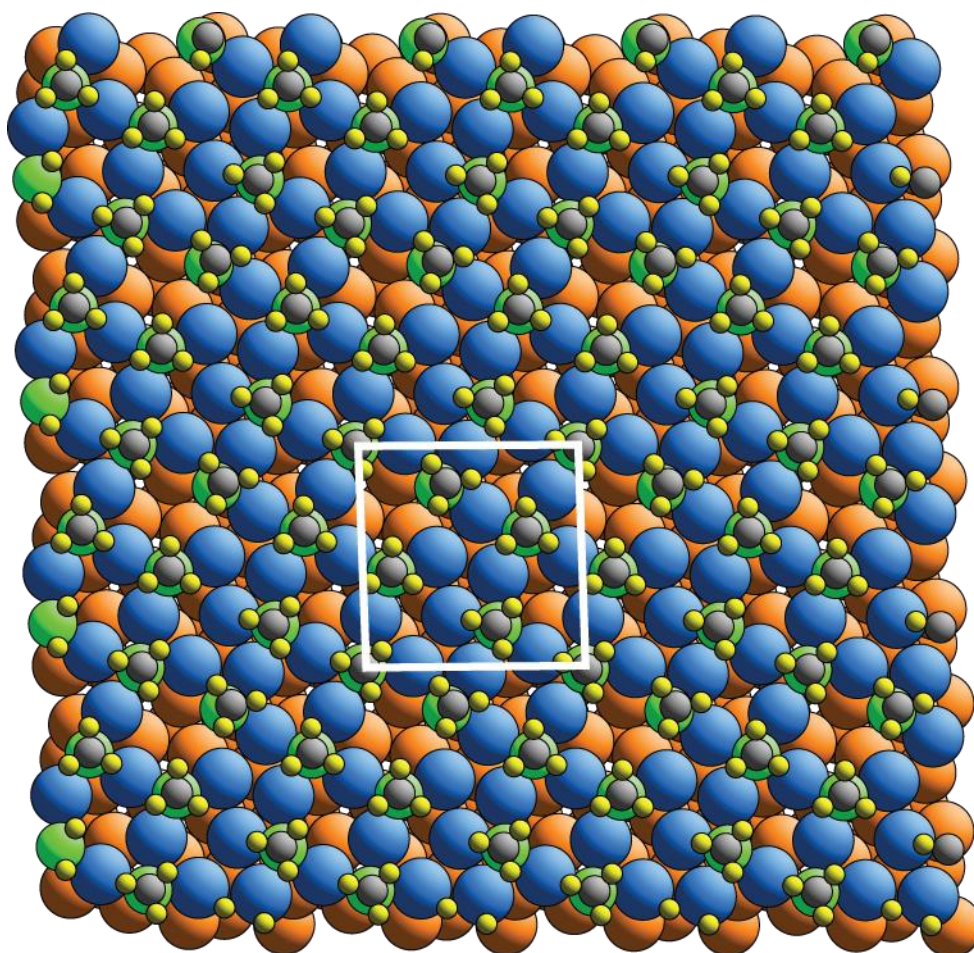


Fig. 3. Plan view of the ‘reconstruction A’ model of the Cu(111)/CH₃S surface obtained by relaxing the atomic positions in the ideal pseudo-(100) reconstruction model. The atom colouring is as in Fig. 1 apart from the Cu atoms in the reconstructed overlayer which are depicted by blue spheres with the same radius as the (gold) Cu substrate atoms.

The white lines show the $\begin{matrix} 4 \\ \text{M} \\ 3 \end{matrix}$ $\begin{matrix} 3 \\ \text{f} \\ 3 \end{matrix}$ unit mesh.

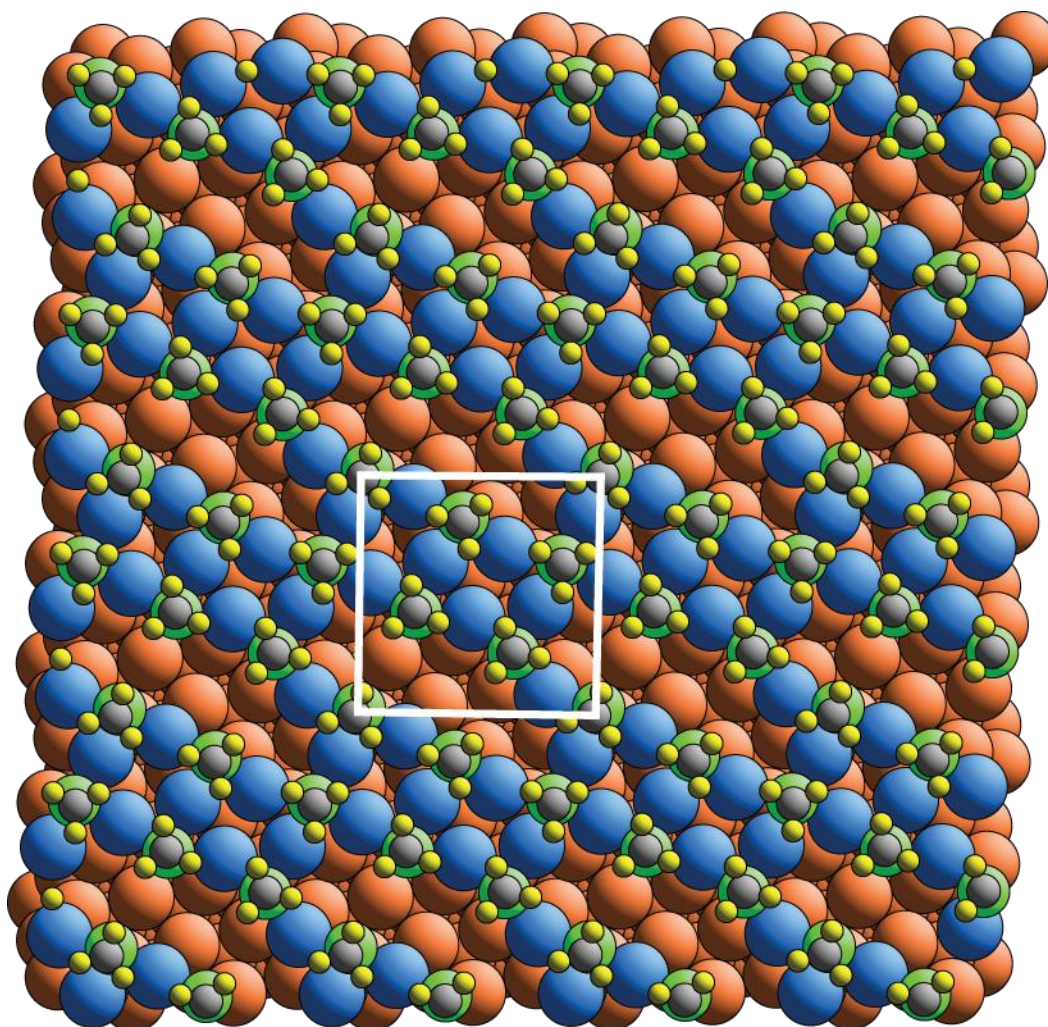


Fig. 4. Plan view of the 'reconstruction G' model of the Cu(111)/CH₃S surface. The atom colouring is as in Fig. 3. The white lines show the $\begin{Bmatrix} 4 \\ 3 \\ 3 \end{Bmatrix}$ unit mesh.

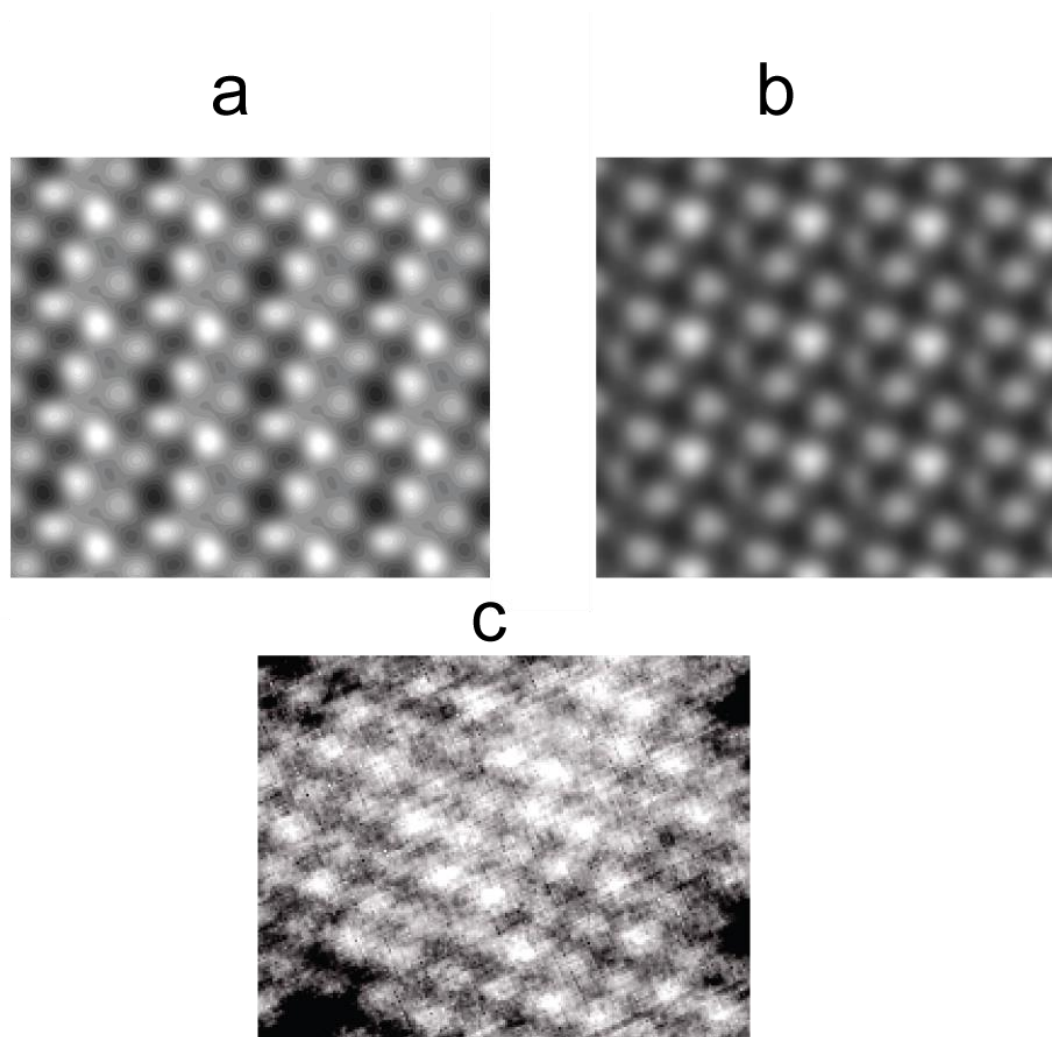


Fig. 5 Simulated STM images from (a) reconstruction A and (b) reconstruction G compared with the experimental image (c) adapted from ref [3].

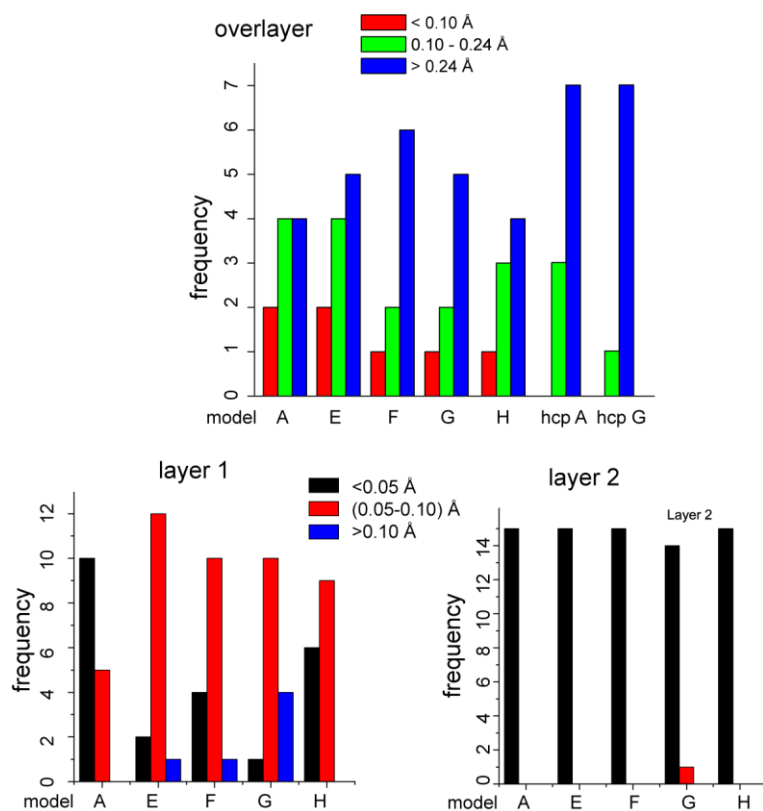
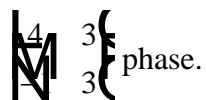


Fig. 6 Histograms of the distribution of lateral offsets of Cu atoms in the outermost atomic layers from bulk-termination sites for five different reconstruction models of the



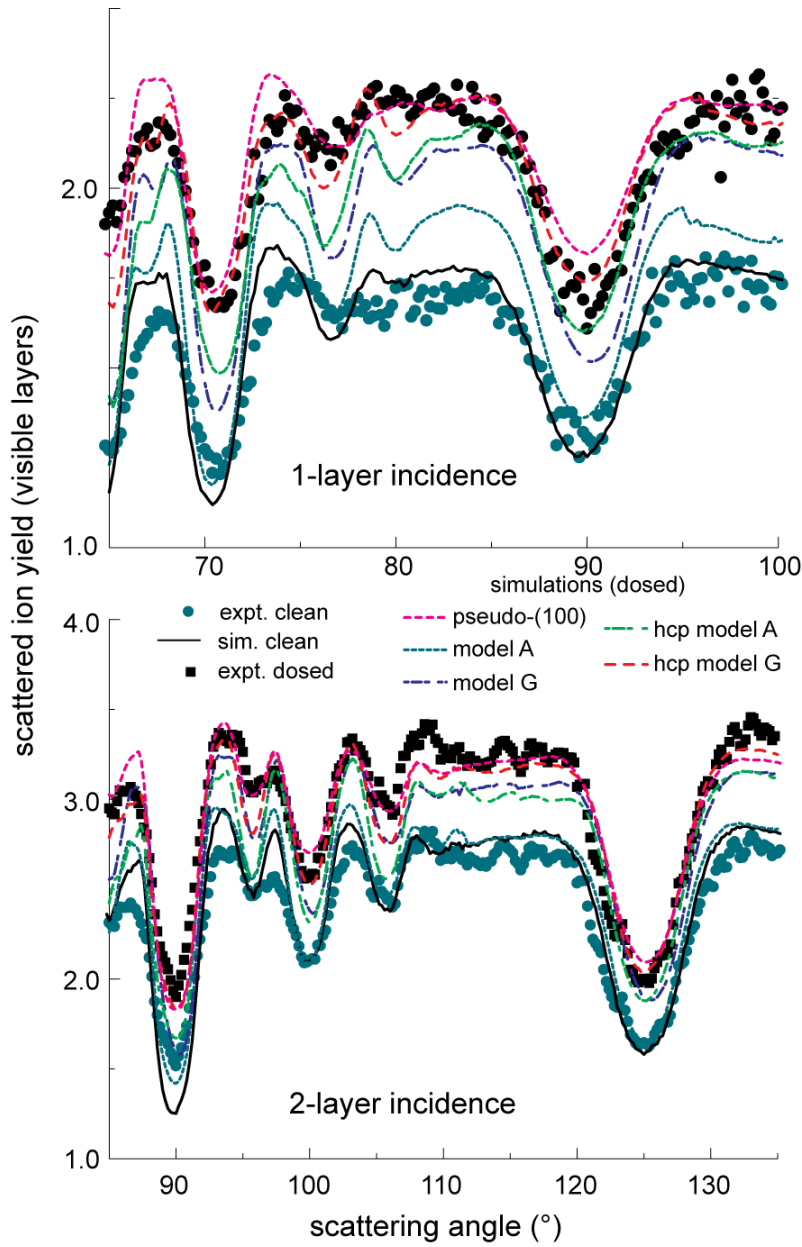


Fig. 7. Comparison of the MEIS experimental blocking curves [5], recorded in two different incident directions, from clean and thiolate-covered Cu(111), with the results of VEGAS simulations for different structural models of the surface structure.

References

- 1 D.P.Woodruff, Phys. Chem. Chem. Phys. 10 (2008) 7211
- 2 N.P.Prince, D.L.Seymour, D.P.Woodruff, R.G.Jones, W.Walter Surf. Sci. 215 (1989) 566
- 3 S.M. Driver, D.P. Woodruff, Surf. Sci. 457 (2000) 11.
- 4 D.P. Woodruff, J. Phys.: Condens. Matter, 6, (1994) 6067.
- 5 G.S. Parkinson, M.A. Muñoz-Márquez, P.D. Quinn, M.J. Gladys, D.P. Woodruff, P. Bailey, T.C.Q. Noakes, Surf. Sci. 598 (2005) 209.
- 6 S.M. Driver, D.A. King, Surf. Sci. 601 (2007) 510.
- 7 A. Imanishi, S. Takenaka, T. Yokoyama, Y. Kitajima, T. Ohta, J. Phys. IV France, 7 (1997) C2-701.
- 8 M.S. Kariapper, C. Fisher, D.P. Woodruff, B.C.C. Cowie, R.G. Jones, J. Phys.; Condens. Matter 12 (2000) 2153.
- 9 H. Kondoh, N. Saito, F. Matsui, T. Yokoyama, T. Ohta, H. Kuroda, J. Phys. Chem. B 105 (2001) 12870.
- 10 S. Vollmer, P. Fouquet, G. Witte, Ch Boas, M. Kunat, U.Burghaus, C. Wöll, Surf. Sci. 462 (2000) 135.
- 11 S. Vollmer, G. Witte, Ch. Wöll, Langmuir 17 (2001) 7560.
- 12 F. Allegretti, F. Bussolotti, D. P. Woodruff, V. R. Dhanak, M. Beccari, V. Di Castro, M.G. Betti, C. Mariani, Surf. Sci. 602 (2008) 2453
- 13 S.M. Driver, D.P. Woodruff, Surf. Sci. 488 (2001) 207.
- 14 F. Bussolotti, V. Corradini, V. Di Castro, M.G. Betti, C.Mariani, Surf. Sci. 566–568 (2004) 591
- 15 D.C. Sheppard, M. Walker, C.F. McConville, D.P. Woodruff, T.C.Q. Noakes, P. Bailey, Surf. Sci. 604 (2010) 1727.
- 16 A. Ferral, E.M. Patrito, P. Paredes-Olivera. J. Phys. Chem. B 110 (2006) 17050.
- 17 H. Grönbeck, J.Phys.Chem. C 114 (2010) 15973.
- 18 P. Seema, J. Behler, D. Marx, J. Phys. Chem. C 117 (2013) 337.

-
- 19 S.J. Clark, M.D. Segall, C.J. Pickard, P.J. Hasnip, M.J. Probert, K. Refson, M.C. Payne, Z. Krist., 220 (2005) 567.
- 20 B. Hammer, L.B. Hansen, J.K. Norskov, Phys. Rev. B, 59 (1999) 7413.
- 21 O.H. Nielsen, R.M. Martin, Phys. Rev. B 32 (1985) 3780.
- 22 T. Tsuduki, A. Imanishi, K. Isawa, S. Terada, F. Matsui, M. Kiguchi, T. Tokoyama, T. Ohta, J. Synchrtron Rad. 6 (1999) 787.
- 23 M.J. Harrison, D.P. Woodruff, J. Robinson, Surf. Sci. 602 (2008) 226.
- 24 J. Tersoff, D.R. Hamann, Phys. Rev. B 31 (1985) 805.
- 25 J.F. van der Veen, Surf. Sci. Rep. 5 (1985) 199
- 26 R.M. Tromp, J.F. van der Veen, Surf. Sci. 133 (1983) 159.
- 27 T. Okazawa, F. Takeuchi, Y. Kido, Phys. Rev. B (2005) 075408.
- 28 D.P. Woodruff, J. Robinson, J. Phys.: Condens. Matter 12 (2000) 7699.